Solving Standard and Generalized EMPM Eigenvalue Problems: A QUBO Approach for the D-Wave Quantum Annealer

G. De Gregorio[1,2], *C.* De Lucia[3], *A.* Martone[3], *F.A.* D'Aniello[3], *A.* Mastroianni[2], *G.* Nunziata[2], *F.* Knapp[4], *N.* Lo Iudice[5], and *P.* Veselý[6]

[1]Dipartimento di Matematica e Fisica, Università degli Studi della Campania "Luigi Vanvitelli", viale Abramo Lincoln 5, I-81100 Caserta, Italy
[2]Istituto Nazionale di Fisica Nucleare, Complesso Universitario di Monte S. Angelo, Via Cintia, I-80126 Napoli, Italy
[3]Centro Italiano Ricerche Aerospaziali (CIRA), Via Maiorise, 81043 Capua, CE, Italy
[4]Institute of Particle and Nuclear Physics, Faculty of Mathematics and Physics, Charles University, V Holešvičkách 2, 180 00 Prague, Czech Republic
[5]Dipartimento di Fisica, Università di Napoli Federico II, 80126 Napoli, Italy
[6]Nuclear Physics Institute, Czech Academy of Sciences, 250 68 Řež, Czech Republic

Abstract. Within the Equation of Motion Phonon Method (EMPM) framework, we address the computation of the ground-state eigenpair of nuclear Hamiltonians by reformulating the eigenvalue problem as a Quadratic Unconstrained Binary Optimization (QUBO). To this end, we adopt a QUBO-based iterative steepest-descent algorithm and validate its performance using Simulated Annealing, demonstrating its feasibility for nuclear many-body calculations. This work represents a first step toward implementations on quantum annealers and extensions to the full eigenspectrum.

1 Introduction

In nuclear physics, many-body methods often require the solution of large eigenvalue problems. A notable example is the Equation of Motion Phonon Method [1–5], developed for the spectroscopy of atomic nuclei at low and high energies. EMPM starts from an Hartree-Fock (HF) basis to construct an orthonormal multiphonon basis from Tamm–Dancoff (TD) phonons, reducing the complexity of the Hamiltonian while preserving the Pauli principle and treating one- and multiphonon states consistently. Despite these advantages, the diagonalization of the resulting matrices remains computationally demanding.

To address this challenge, quantum computing offers novel strategies. By exploiting qubits, which can exist in superposition and can be entangled, quantum algorithms exploit interference and quantum parallelism to tackle problems difficult for classical machines [6]. Although practical limitations persist—such as limited qubit numbers, noise, and error correction [7]—specialized algorithms have been developed for near-term devices.

Here we investigate a QUBO-based iterative steepest-descent algorithm [8], designed to compute the lowest eigenpair of a symmetric matrix through quantum annealing [9, 10].

Quantum annealing is well-suited to optimization tasks and provides an alternative to the phase estimation algorithm [6], which remains impractical on current hardware.

This work applies the algorithm to EMPM eigenvalue problems, using Simulated Annealing to validate its performance. A comparison with Quantum Annealing and the extension to compute the full eigenspectrum are left for future work.

2 The EMPM: A brief outline

The basic ingredients of the EMPM are the HF particle-hole (p-h) vacuum $|0\rangle$ and the TD states $|\lambda\rangle = O^\dagger_\lambda |0\rangle$ of energy E_λ, where

$$O^\dagger_\lambda = \sum_{ph} c^\lambda_{ph} (a^\dagger_p \times b_h)^\lambda \tag{1}$$

is the phonon operator built out of the creation and annihilation operators $a^\dagger_p = a^\dagger_{x_p j_p m_p}$ and $b_h = (-)^{j_h+m_h} a_{x_h j_h -m_h}$, which are coupled to spin J_λ.

Starting from $|0\rangle$ and the TD one-phonon states $|\lambda\rangle$, we intend to generate iteratively an orthonormal basis of n-phonon ($n = 2, 3..$) correlated states $|\beta\rangle = |\alpha_n\rangle$ assuming known the $(n-1)$-phonon basis states $|\alpha\rangle = |\alpha_{n-1}\rangle$ of energy E_α. To this purpose we construct the set of redundant states

$$\left|(\lambda \times \alpha)^\beta\right\rangle = \left\{O^\dagger_\lambda \times |\alpha\rangle\right\}^\beta \tag{2}$$

and extract from them a basis of linearly independent states by resorting to the Cholesky decomposition method. We are then allowed to write the n-phonon states we search for in the expanded form

$$|\beta\rangle = \sum_{\lambda\alpha} C^\beta_{\lambda\alpha} \left|(\lambda \times \alpha)^\beta\right\rangle . \tag{3}$$

They can be determined by solving the generalized eigenvalue equation within the n-phonon subspace. This equation can be written as

$$\mathcal{H}C = (\mathcal{A}\mathcal{D})C = E\mathcal{D}C, \tag{4}$$

or, more explicitly,

$$\sum_{\lambda'\alpha'} \mathcal{H}^\beta_{\lambda\alpha\lambda'\alpha'} C^\beta_{\lambda'\alpha'} = E_\beta \sum_{\lambda'\alpha'} \mathcal{D}^\beta_{\lambda\alpha\lambda'\alpha'} C^\beta_{\lambda'\alpha'}, \tag{5}$$

where $\mathcal{D}$ is the overlap or metric matrix which preserves the Pauli principle and $\mathcal{A}$ is a matrix containing the phonon-phonon interaction whose explicit expression can be found, for instance, in Ref. [4]. The solution of Eq. 5 yields the n-phonon basis states (Eq. 3). The iteration of the procedure up to an arbitrary n produces a set of states which, added to HF ($|0\rangle$) and TD ($\{|\alpha_1\rangle\} = \{|\lambda\rangle\}$), form an orthonormal basis $\{|\alpha_n\rangle\}$ ($n = 0, 1, 2, 3, ...$). Such a basis is then adopted to solve the eigenvalue problem in the full space

$$\sum_{\alpha_n\beta_{n'}} \Big((E_{\alpha_n} - \mathcal{E}_\nu)\delta_{\alpha_n\beta_{n'}} + \mathcal{V}_{\alpha_n\beta_{n'}}\Big) C^\nu_{\beta_{n'}} = 0, \tag{6}$$

where $\mathcal{V}_{\alpha_n\beta_{n'}}$ is the coupling among different phonon spaces, and is null for $n' = n$. Its expression can be found for example in Ref. [4]. The solution of the final eigenvalue equation (Eq. 6) yields the eingenalues $\mathcal{E}_\nu$ and the corresponding eigenvectors ($n = 0, 1, 2, 3....$)

$$|\Psi_\nu\rangle = \sum_{n,\alpha_n} C^\nu_{\alpha_n} |\alpha_n\rangle . \tag{7}$$

3 QUBO-based algorithm

We now outline a QUBO-based algorithm for computing the lowest eigenpair, more details can be found in Ref. [8]. Let A be symmetric. By the spectral theorem, the smallest eigenvalue λ and the corresponding eigenvector $\mathbf{v}$ minimize the Rayleigh quotient $\langle x|\,A\,|x\rangle\,/\,\langle x|x\rangle$, namely

$$\lambda = \min_{\|\mathbf{x}\|=1} \langle x|\,A\,|x\rangle\,, \quad |v\rangle = \arg\min_{\|\mathbf{x}\|=1} \langle x|\,A\,|x\rangle\,. \tag{8}$$

The proposed approach employs a binary representation of the variables, and is structured in two distinct phases: an initial guess phase followed by an iterative descent phase.

Let's start from the first step. To approximate real variables, each x is expressed via b bits using the precision vector

$$\boldsymbol{\rho} = \left(-1, \tfrac{1}{2}, \tfrac{1}{2^2}, \ldots, \tfrac{1}{2^{b-1}}\right), \tag{9}$$

through

$$x = \boldsymbol{\rho} \cdot \mathbf{x_b}. \tag{10}$$

The set of all the real values we can obtain is $C_{n,b} := \left\{(I_n \otimes \boldsymbol{\rho})\,\mathbf{x}_b \mid \mathbf{x}_b \in \{0,1\}^{nb}\right\}$, for n variables. Now, if Q is a symmetric matrix, and r an n-dimentional vector, a quadratic programming problem

$$\arg\min_{\mathbf{x}\in[-1,1]^n} \mathbf{r}^t\mathbf{x} + \mathbf{x}^t Q\mathbf{x}, \tag{11}$$

is approximated as a QUBO over $C_{n,b}$, yielding

$$\arg\min_{\mathbf{x}\in C_{n,b}} \mathbf{r}^t\mathbf{x} + \mathbf{x}^t Q\mathbf{x} \tag{12}$$

or, equivalently,

$$\arg\min_{\mathbf{x}_b\in\{0,1\}^{(n\cdot b)}} \mathbf{x}_b^t(\mathrm{Diag}(\mathbf{r}I_n \otimes \boldsymbol{\rho}) + Q \otimes P)\mathbf{x}_b. \tag{13}$$

where P is the precision matrix $P = \boldsymbol{\rho}^t\boldsymbol{\rho}$. In summary, with b bits the real optimization problem in n variables is approximated by a QUBO of size $n \cdot b$. This construction is not restricted to the cube $[-1,1]^n$: for $[-\delta,\delta]^n$ one simply rescales the precision vector by δ.

The first phase of the algorithm, is the initial guess phase. If $\lambda_1 \le \lambda_2 \le \ldots. \le \lambda_n$, to approximate λ_1, we solve

$$\arg\min_{\mathbf{x}\in C_{n,b}} \langle\mathbf{x}|\,A\,|\mathbf{x}\rangle\,. \tag{14}$$

If A positive definite, this yields trivial $|0\rangle$, this can be overcome minimizing

$$\langle\mathbf{x}|\,(A - \lambda I_n)\,|\mathbf{x}\rangle\,. \tag{15}$$

The algorithm starts with λ initialized as $\mathrm{tr}(A)/n$ [8]. Then, solve Eq.15 to obtain v_1, update λ using the Rayleigh quotient $\lambda = \frac{v_1^T A v_1}{\|v_1\|^2}$ and solve Eq.15 again, possibly biasing with v_1, to obtain v_2, and repeat until λ stabilizes. We get the eigenvalue λ_1 with a relatively large error (2-3 digits).

Then, once the initial guess phase has come to an end, the algorithm enters a descent stage where the precision can be increased to essentially arbitrary order. To illustrate this, consider a function $f : \mathbb{R}^m \to \mathbb{R}$ we want to minimize, it can be Taylor expanded around the initial guess $\mathbf{x}_0$, and gives

$$f(\mathbf{x}) \approx f(\mathbf{x}_0) + \nabla f \cdot \delta + \tfrac{1}{2}\,\langle\delta|\,\mathcal{H}e(f)\,|\delta\rangle\,, \tag{16}$$

where ∇f and $\mathcal{H}e(f)$ represent the gradient and the Hessian of f. One may choose $\delta = \mathbf{x} - \mathbf{x_0}$ to minimize $\nabla f \cdot \delta$ (gradient descent) or $\nabla f \cdot \delta + \frac{1}{2}\delta^T\mathcal{H}e(f)\delta$ (second-order methods such as

Newton, BFGS, Newton-CG). After updating $x_1 = x_0 + \delta$, the process is repeated by Taylor expansion around x_1. The algorithm, in its descendent phase, uses a QUBO to obtain good approximations to

$$\arg\min_{\delta \in C_{n,b}} \nabla f \cdot \delta + \tfrac{1}{2}\delta^T \mathcal{H}e(f)\delta. \tag{17}$$

As in Newton-CG [11] or BFGS [11], it requires computing (but not inverting) the Hessian, and benefits from a line search. Here, line search reduces to minimizing a quadratic, so the optimal scaling is directly computable. If x_k is already closer to the true solution than any point in the discretized cube, QUBO minimization cannot improve it. To avoid stagnation, the descent phase enforces a minimum step size with line search. If the candidate x_{k+1} is worse, it is discarded and the cube $C_{n,b}$ is rescaled to $p \cdot C_{n,b}$ with $p < 1$, i.e., repeating the construction outlined with precision vector $p \cdot \boldsymbol{\rho}$. The algorithm then proceeds with the smaller cube.

This algorithm can be easily generalized for solving a generalized eigenvalue problem of the form $A\mathbf{v} = \lambda D\mathbf{v}$ with D positive defined: initialize

$$\lambda = \frac{\langle w| A |w\rangle}{\langle w| D |w\rangle} \tag{18}$$

for random $|w\rangle$, replace each Rayleigh quotient with the generalized one, and update $H = A - \lambda D$.

4 Results

As a study case, we consider ^{4}He. The starting Hamiltonian is defined as

$$H = T_{\text{int}} + V_D. \tag{19}$$

Here, T_{int} denotes the intrinsic kinetic energy, and V_D is the Daejeon interaction derived from the *NN* component of the N3LO potential [12] through a two-step procedure. First, the *NN* potential is softened using the SRG method [13] with flow parameter $\lambda = 1.5$ fm^{-1}; then, a phase-equivalent transformation is applied to determine an optimal parametrization of the *NN* force. We use this Hamiltonian to generate a HF basis encompassing 3 major shells. We use the HF states to create the TD phonon basis and generate the 2-phonon basis by deriving and solving iteratively the EMPM Eq. 4; the basis so constructed is adopted to solve the final eigenvalue problem in the multiphonon space (Eq. 6).

We consider the standard eigenvalue problems—namely, the Tamm-Dancoff diagonalization and the full EMPM eigenvalue problem (Eq. 6)—as well as the generalized EMPM eigenvalue problem (Eq. 4), all for $J^\pi = 2^+$. The matrix dimensions differ in each case and are specified below.

Tamm–Dancoff

For the TD case, the matrix corresponding to $J^\pi = 2^+$ has dimension $d = 8$. Calculations are performed for different numbers of bits $b = 2, 4, 6, 8$. The starting point shown in the plots corresponds to the output of the initial guess phase, where the parameter *precision* (p) (see Section 3) is set to 1. The plots show the evolution of the eigenvalue error (*eval_error*) and eigenvector error (*evec_error*) as functions of the precision parameter (p) and the number of iterations. Here, *eval_error* and *evec_error* are defined as the differences between the computed eigenvalue and eigenvector and their corresponding true values, with the latter evaluated in terms of the Euclidean distance. The reference eigenvalues and eigenvectors were obtained using standard numerical solvers.

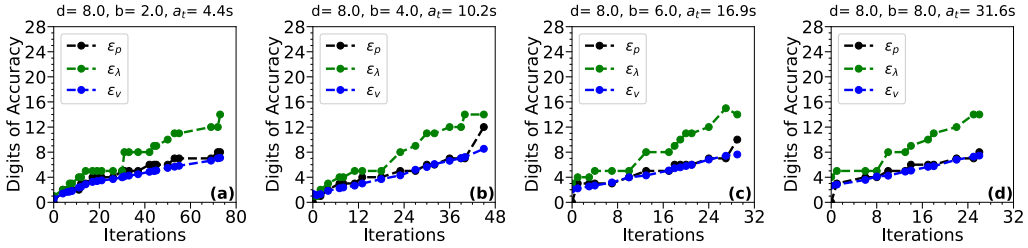

Figure 1: Digits of accuracy of the lowest eigenvalue ($\varepsilon_\lambda = -log_{10}(eval\_error)$) and of the correspondent eigenvector ($\varepsilon_v = -log_{10}(evec\_error)$) of the TD eigenvalue problem for $J^\pi = 2^+$. The value $\varepsilon_p = -log_{10}(p)$, is also reported for completeness.

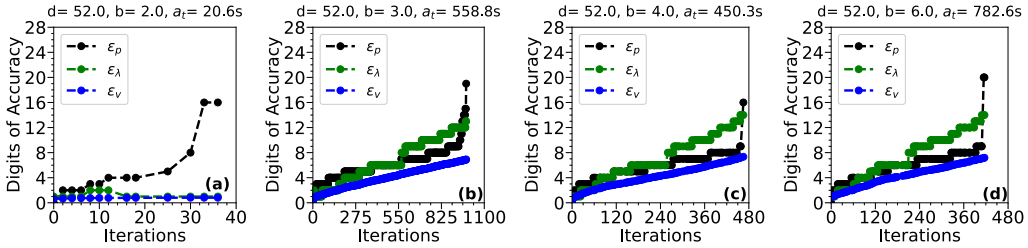

Figure 2: Same as Fig. 1 in the case of the full Hamiltonian up to two phonons.

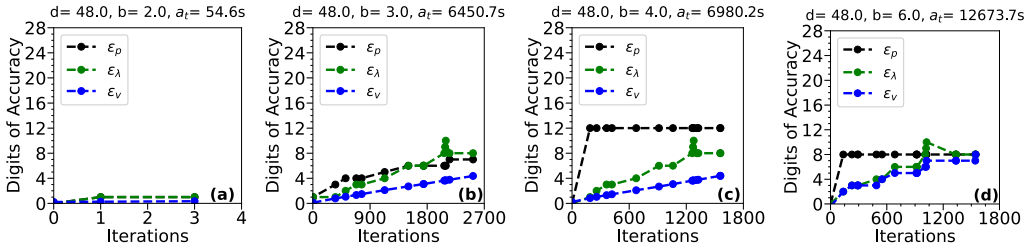

Figure 3: Same as Fig. 1 in the case of the EMPM generalized eigenvalue problem.

This illustrates how quickly and by how much the accuracy of the lowest-energy eigenpair improves during the descent phase of the algorithm as the discretized cube over which the minimization occurs is refined by tuning p.

Finally, the annealing time (a_t) represents the total computational time spent by the algorithm to solve the QUBO problem. In the case under investigation, this time depends not only on the computational resources of the server used for the simulations — which is kept fixed to ensure a fair comparison — but also on the `num_reads` parameter of the Simulated Annealing algorithm implemented in the `PyQUBO` library.

The `num_reads` parameter specifies the number of independent runs of the Simulated Annealing process performed by the solver; each read corresponds to a single stochastic realization of the annealing process, producing one candidate solution. Increasing `num_reads` im-

proves the probability of obtaining lower-energy configurations, but proportionally increases a_t.

In this study, `num_reads` is fixed to 100 for all simulations. Different values of this parameter, as well as a different computational backend, would lead to different absolute values of a_t. For this reason, a_t is reported and discussed only in a *relative* sense, allowing a consistent comparison across different configurations under identical computational conditions.

Let us analyze the dependence of the number of iterations N_{it} on b. For $b = 2$, $N_{it} \simeq 75$, while for $b = 8$, $N_{it} \simeq 25$. The annealing time increases with b, ranging from 4.4 s to 31.6 s. In all cases, the number of accurate digits in the eigenvector grows almost linearly with the number of iterations, from $\simeq 2$ up to $\simeq 8$, once the thirteenth digit of precision is reached for the eigenvalue.

Full eigenvalue problem

For the full Hamiltonian (Eq. 6), the matrix dimension is $d = 52$. The results are reported in Figure 2. Here, no improvement is observed for $b = 2$ with respect to the initial guess phase result. For higher b, the iterative method achieves machine-precision accuracy for the lowest eigenvalue within $N_{it} = 1000$ for $b = 3$ and $N_{it} = 500$ for $b = 6$. The corresponding annealing times are 20.6 s and 782.6 s, respectively. These results indicate that larger matrices require a higher minimum number of bits to reach machine precision.

Generalized eigenvalue problem

For the generalized eigenvalue problem (Eq. (4)) with $n = 2$ phonons, we have a matrix dimension of $d = 48$. We adopt the QUBO-based algorithm, adjusted for generalized eigenvalue problems as described in Section 3. The robustness of the algorithm is tested for $b = 2, 3, 4, 6$.

For $b = 2$ (Figure 3), as for the full eingevalue problem case previously discussed, no gain in accuracy is observed with respect to the value obtained at the end of the initial guess phase. The increased matrix dimension highlights how the number of iterations required to reach 8-digit accuracy in the eigenvalues decreases from $\simeq 2100$ to 1000 as b increases from 2 to 6 (Figures 3(a)–(d)). Conversely, the annealing time a_t grows from 6450.7 s to 12673.7 s when moving from $b = 2$ to $b = 6$.

From a detailed comparison between the results obtained for the standard eigenvalue problem (Fig. 2) and for the generalized one (Fig. 3), two main differences can be observed. First, the final precision reached in the two cases is not the same; second, the total annealing time a_t differs, despite the similar problem dimension.

In the case of generalized eigenvalue problems, the numerical results indicate that it is no longer possible to achieve double-precision machine accuracy for the eigenvalue. The highest accuracy attainable is of the order of 10^{-8}. This limitation is intrinsic to the nature of the generalized eigenvalue problem itself, rather than a shortcoming of the QUBO-based eigensolver. Indeed, the `eig` routine from the `scipy.linalg` library [14], used to compute the reference generalized eigenpair, relies on different LAPACK (Linear Algebra PACKage) algorithms [15] depending on whether the metric matrix D is the identity (standard case) or not (generalized case). For generalized case, the attainable numerical precision decreases, and the computed eigenvalues are accurate up to roughly 8–10 significant digits.

Regarding the difference in the annealing time a_t, this originates from the increased complexity associated with a non-orthonormal basis. This is reflected, for instance, in a larger number of iterations required to reach the highest possible precision.

Conclusions

We have investigated a QUBO-based iterative steepest-descent algorithm for computing the lowest eigenpair of nuclear Hamiltonians within the EMPM framework. Validation using Simulated Annealing demonstrates that the algorithm systematically improves both eigenvalue and eigenvector accuracy, with convergence rates strongly dependent on the number of bits b and the precision parameter.

In the TD case, small matrices ($d = 8$) reach high accuracy within a limited number of iterations, showing rapid improvement of eigenvector digits. For larger matrices ($d = 52$), a higher minimum number of bits is required to attain machine precision, with the number of iterations and annealing time increasing accordingly. Similarly, for generalized eigenvalue problems ($d = 48$), the method remains robust, although larger matrices demand more iterations and longer annealing times to achieve the desired accuracy.

Overall, the algorithm proves effective across different matrix sizes and problem types, providing a viable route for future implementations on quantum annealers and potential extensions to compute the full eigenspectrum of nuclear Hamiltonians.

Acknowledgments

G. De Gregorio acknowledge the support by EU-FESR, PON Ricerca e Innovazione 2014-2020- DM 1062/2021, and the collaboration with Giovanni Frattini, and the company partner of the project Engineering Ingegneria Informatica.

References

[1] G. De Gregorio, J. Herko, F. Knapp, N. Lo Iudice, P. Veselý, Ground-state correlations within a nonperturbative approach, Phys. Rev. C **95**, 024306 (2017). 10.1103/PhysRevC.95.024306

[2] G. De Gregorio, F. Knapp, N. Lo Iudice, P. Veselý, Microscopic multiphonon approach to spectroscopy in the neutron-rich oxygen region, Phys. Rev. C **97**, 034311 (2018). 10.1103/PhysRevC.97.034311

[3] G. De Gregorio, F. Knapp, N. Lo Iudice, P. Veselý, Removal of the center of mass in nuclei and its effects on ^{4}He, Physics Letters B **821**, 136636 (2021). https://doi.org/10.1016/j.physletb.2021.136636

[4] G. De Gregorio, F. Knapp, N. Lo Iudice, P. Veselý, Spectroscopic properties of ^{4}He within a multiphonon approach, Phys. Rev. C **105**, 024326 (2022). 10.1103/PhysRevC.105.024326

[5] F. Knapp, P. Papakonstantinou, P. Veselý, G. De Gregorio, J. Herko, N. Lo Iudice, Comparative analysis of formalisms and performances of three different beyond-mean-field approaches, Phys. Rev. C **107**, 014305 (2023). 10.1103/PhysRevC.107.014305

[6] M.A. Nielsen, I.L. Chuang, Quantum Computation and Quantum Information (Cambridge University Press, 2000)

[7] J. Preskill, Quantum Computing in the NISQ era and beyond, Quantum **2**, 79 (2018). 10.22331/q-2018-08-06-79

[8] B. Krakoff, S.M. Mniszewski, C.F.A. Negre, Controlled precision qubo-based algorithm to compute eigenvectors of symmetric matrices, PLOS ONE **17**, 1 (2022). 10.1371/journal.pone.0267954

[9] M. Illa, M.J. Savage, Basic elements for simulations of standard-model physics with quantum annealers: Multigrid and clock states, Physical Review A **106**, 052605 (2022). 10.1103/PhysRevA.106.052605

[10] G.T. Balducci, B. Chen, M. Möller, M. Gerritsma, R.D. Breuker, Review and perspectives in quantum computing for partial differential equations in structural mechanics, Frontiers in Mechanical Engineering **8**, 914241 (2022). 10.3389/fmech.2022.914241

[11] J. Nocedal, S.J. Wright, Numerical Optimization, 2nd edn. (Springer, New York, 2006), ISBN 978-0387-30303-1

[12] A. Shirokov, I. Shin, Y. Kim, M. Sosonkina, P. Maris, J. Vary, N3LO NN interaction adjusted to light nuclei in ab exitu approach, Physics Letters B **761**, 87 (2016). https://doi.org/10.1016/j.physletb.2016.08.006

[13] F. Wegner, Flow-equations for hamiltonians, Annalen der Physik **506**, 77 (1994), `https://onlinelibrary.wiley.com/doi/pdf/10.1002/andp.19945060203`. https://doi.org/10.1002/andp.19945060203

[14] P. Virtanen, R. Gommers, T.E. Oliphant, M. Haberland, T. Reddy, D. Cournapeau, E. Burovski, P. Peterson, W. Weckesser, J. Bright et al., Scipy 1.0: Fundamental algorithms for scientific computing in python, Nature Methods **17**, 261 (2020). 10.1038/s41592-019-0686-2

[15] Lapack users' guide, https://www.netlib.org/lapack/lug/lapack_lug.html